DENTAL MATERIALS 35 (2019) 1279–1290

Available online at www.sciencedirect.com

ScienceDirect

journal homepage: www.intl.elsevierhealth.com/journals/dema

Silane influence on bonding to CAD-CAM composites: An interfacial fracture toughness study

Maher Eldafrawy[a], *Laura Greimers*[a], *Sandrine Bekaert*[a,b], *Patrick Gailly*[c], *Cédric Lenaerts*[c], *Jean-François Nguyen*[d,e], *Michaël Sadoun*[f], *Amélie Mainjot*[a,b,*]

[a] *Dental Biomaterials Research Unit (d-BRU), Institute of Dentistry, University of Liège (ULiège), Liège, Belgium*
[b] *Department of Fixed Prosthodontics, Institute of Dentistry, University of Liège Hospital (CHU), Liège, Belgium*
[c] *Surface Micro and Nano Engineering Division, Centre spatial de Liège, University of Liège (ULiège), Liège, Belgium*
[d] *UFR d'Odontologie, Université Paris Diderot, Paris, France*
[e] *PSL Research University, Chimie ParisTech-CNRS, Institut de Recherche de Chimie Paris, Paris, France*
[f] *MaJEB sprl, Liège, Belgium*

ARTICLE INFO

Article history:
Received 15 February 2019
Received in revised form
21 May 2019
Accepted 22 May 2019

Keywords:
Dental materials
Prosthetic dentistry
Dental prosthesis retention
Polymer-infiltrated ceramic network
Composite cement
High-temperature high-pressure polymerization
Fracture mechanics
Notchless triangular prism test
Surface roughness
Biomaterials

ABSTRACT

Objectives. To evaluate silane influence on the interfacial fracture toughness (IFT) of composite cement, with the two sub-classes of CAD-CAM composites, polymer-infiltrated ceramic networks (PICN) and dispersed fillers (DF), after hydrofluoric acid etching (HF) or airborne-particle abrasion (AB). A secondary objective was to correlate results with developed interfacial area ratio (Sdr) and surface wettability.

Methods. Experimental PICN and DF blocks were cut into equilateral half-prisms, which were treated with HF or AB, then treated with an experimental silane or not and bonded to their counterparts with an experimental light-cure resin cement. After thermocycling, samples (n = 30 per group) were tested for IFT using the notchless triangular prism test in a water bath at 36 °C. Moreover, profilometry and contact angle measurement were performed on rectangular samples of each group. Finally, bonding interface was analysed by SEM.

Results. PICN-HF treated with silane showed the highest IFT significantly. Three-way ANOVA revealed the influence of silane, material class and surface pre-treatment (HF or AB) on IFT ($p < 0.05$). When silane was used, IFT was correlated with Sdr, while surface wettability was increased. Silane application significantly increased IFT for PICN but not for DF, while PICN performed better with HF and DF with AB.

Significance. Silane increases IFT of composite cement with PICNs, but not with DF materials. Results suggest that silane increases the micromechanical bond by promoting resin cement spreading and penetration in surface roughness. This roughness is significantly higher for pre-treated PICNs than for DF due to their specific honeycomb microstructure when etched, which explains their better bonding properties.

* *Corresponding author at:* Dental Biomaterials Research Unit (d-BRU) and Department of Fixed Prosthodontics, Institute of Dentistry, University of Liège (ULiège) and University of Liège Hospital (CHU), 45 Quai G. Kurth, Liège, 4020, Belgium.
E-mail address: a.mainjot@chuliege.be (A. Mainjot).
https://doi.org/10.1016/j.dental.2019.05.019
0109-5641/

1. Introduction

New advances in CAD-CAM processes and related materials allow for the realization of bonded restorations in high-performance composite materials, which exhibit better machinability than ceramics and are able to be milled at very low thickness, offering interesting perspectives in terms of minimally-invasive treatments [1–3]. However, there is a need to study their bonding properties [4] and the mechanism of composite cement adhesion to the material's surface, depending on material composition and microstructure [4].

According to the microstructure, CAD-CAM composites can be sub-classified into dispersed fillers (DF) and polymer-infiltrated ceramic networks (PICN). While DF consist of inorganic fillers, mainly silica-based glass mixed with an organic matrix, most often of urethane di-methacrylate (UDMA), eventually combined with tri-ethylene glycol di-methacrylate (TEGDMA), polymerized at high temperature (>100 °C), PICNs (also called "hybrid ceramics") consist of monomers secondarily infiltrated into a pre-sintered glass-ceramic scaffold and polymerized under high temperature and pressure (HT-HP) (180 °C–300 MPa) [5] (Fig. 1). This patented HT-HP polymerization process [6] provides a high degree of conversion of PICNs, which is advantageous in terms of improving the mechanical properties and monomer release [7–9], but raises some doubts regarding the chemical bonding between the free monomers and the resin cement [5]. Examples of commercially available DF include Lava Ultimate (3M ESPE, St. Paul, MN, USA), Cerasmart (GC, Tokyo, Japan), Shofu blocks (Shofu Inc., Kyoto, Japan), Tetric CAD (Ivoclar Vivadent, Schaan, Liechtenstein), Katana Avencia (Kuraray Noritake, Tokyo, Japan), Brilliant Crios (Coltene, Göppingen, Germany) and Grandio blocs (Voco, Cuxhaven, Germany), which are different in the amount, size and composition of fillers, as well as the organic matrix, while Vita Enamic (Vita Zahnfabrik, Bad Säckingen, Germany) is the only marketed PICN with 75 vol.% (86 wt.%) glass-ceramic.

The effectiveness of composite cement bonding to materials was suggested to be related to two important parameters, the micromechanical interlocking, promoted by surface roughness, and the chemical bond, promoted by silane application [10]. Regarding classical light-cured indirect composites, increasing surface roughness by airborne-particle abrasion was shown to have a greater effect on bond strength than chemical bonding [4]. For CAD-CAM composite materials, the high degree of conversion of the polymers could be suspected to decrease the potential for a chemical co-polymerization with the resin cement, therefore micromechanical interlocking might be of even greater influence on the adhesive interface performance. Regarding DF CAD-CAM composites, airborne-particle abrasion was previously shown to be more effective than etching in increasing the surface roughness and consequently improving the bonding properties [4,11,12], while on the contrary, PICNs showed significantly higher bond strength results when etched than when treated with airborne-particle abrasion [11,13,14]. Indeed, previous work using fracture mechanics highlighted the influence of CAD-CAM composite microstructure on surface roughness and bonding properties [11]. PICNs have a typical double-network microstructure which results in a honeycomb polymer-based structure after etching, which enhances micromechanical retention with composite cement and yields significantly higher IFT values than DF [11,15], with a direct correlation between IFT and surface roughness (expressed as the developed interfacial area ratio, Sdr) having been highlighted.

On the other hand, silane pre-treatment was shown to have a significant positive effect on glass-ceramics bonding [16] and is recommended for all CAD-CAM composites. At low pH, condensated silane molecules react with each other forming dimers, which then condensate to form siloxane oligomers. Subsequently, a further reaction between silane oligomers leads to the formation of strong siloxane bonds (—Si—O—Si—) on the fitting surface of the substrate [17,18]. Another theory suggested that the mechanism of bond enhancement by silanes is that they improve the wettability of ceramic surfaces and reduce the contact angle of resin cements with ceramics. This could allow the resin cement to penetrate into the micro-roughness created on the surface after etching, resulting in increased micromechanical retention [19].

The bonding properties of CAD-CAM composites have been evaluated in a few studies using microtensile or micro(shear) bond strength tests to measure the influence of the type of pre-treatment, composite cement or material [13,14,20–24]. However, bond strength testing suffers from several drawbacks which may result in inaccuracies in the evaluation of the bond strength as a result of sample preparation after bonding, which leads to an increased number of pre-test failures, as well as problems relating to non-uniform stress distributions. A four-point bending test has been recently introduced to reduce those issues [25–27]. The need for a different and more reliable method for the evaluation of the adhesive interfaces drove some authors to introduce fracture mechanics for evaluating the interfacial fracture toughness (IFT) (K_{1C}) of the adhesive layer [25,26,28–32]. IFT allows for the evaluation of the interfacial properties by stably initiating and propagating a crack through the bonded interface, and measuring the crack-propagation resistance or peeling resistance from the substrate, unlike bond strength testing which evaluates the mechanical strength of the whole assembly [25,30]. Several types of fracture toughness tests have already been implemented with dental materials, such as the indentation fracture; single-edge notched beam; simple edge precracked beam; surface crack in flexure; and the chevron notch short rod or beam test [32–35]. The latter has been modified into various versions adapted to dental samples [29,30,36]. Among these versions, the notchless triangular prism (NTP) test, introduced by Ruse et al. [36], was reported to be a simple method [31] and was previously proposed to evaluate both the fracture toughness of a material and the fracture toughness of bonded interfaces [36,37]. Finite element analysis showed that the maximum tensile stress was concentrated at the tip of the crack [36], providing a good level of control and stable crack growth at a low cross-speed (0.05 mm/min); thus, allowing for reliable measurements and the possibility of performing a fatigue process study, controlling crack propagation for a given K_I. In addition, the NTP does not require a notch prior to testing, only a crack initiation point, therefore minimizing

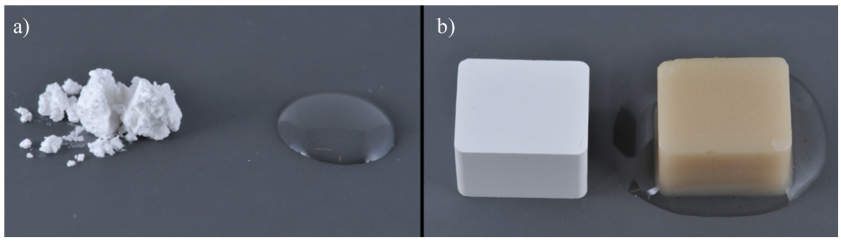

Fig. 1 – (a) Fillers that are incorporated by mixing in a monomer mixture to produce a dispersed filler (DF) composite block. (b) A pre-sintered glass-ceramic scaffold infiltrated with monomer, which is secondarily polymerized under high-temperature and high-pressure to produce a polymer-infiltrated ceramic network (PICN) block. In PICN, glass-ceramic particles are interconnected creating a double-network material (which has a lower content of organic phase than DF).

the bias related to creation of the notch, especially with the low adhesive interface thickness.

Consequently, the main objective of this study was to evaluate the influence of silane on the interfacial fracture toughness (IFT) of composite cement with two sub-classes of CAD-CAM composites, polymer-infiltrated ceramic network (PICN) and dispersed filler (DF), after etching or airborne-particle abrasion. A secondary objective was to correlate the results with developed interfacial area ratio (Sdr) and surface wettability. The null hypotheses are that (1) material class; (2) surface texture after pre-treatment; (3) silane, do not influence IFT.

2. Materials and methods

Experimental blocks of the two classes of CAD-CAM composites, PICN and DF, were manufactured and tested with experimental resin cement and silane. The details of the compositions of all the materials are described below.

2.1. *Experimental material compositions*

2.1.1. *Experimental PICN*

The process of producing the porous ceramic network is described by Nguyen et al. [8]. After sintering, the porous network consisted of 73.8 vol.% slip casted Vita Mark II glass-ceramic powder (Vita Zahnfabrik, 2.6 μm D50 grain size distribution); which were then infiltrated by UDMA and di-*tert*-amyl peroxide (initiator), and polymerized under HT-HP (180 °C–300 MPa) to give the final PICN blocks of 85 wt.% glass ceramic network and 15 wt.% organic component (Fig. 1).

2.1.2. *Dispersed filler resin blocks*

The dispersed filler resin composite blocks were composed of 2:1 (weight) UDMA and TEGDMA, with the addition of 1 wt.% benzoyl peroxide (Aldrich, Darmstadt, Germany) to form the organic part. The mixture was left for 24 h to stabilize.

67 wt.% silanated barium borosilicate glass (0.7 μm) (Esschem Europe, Seaham, England) and 3 wt.% synthetic amorphous organosilane-treated silica (40 nm) (Evonik Industries, Essen, Germany) were added to 30 wt.% of the organic mixture and polymerized under HT-HP, as was done for PICN.

2.1.3. *Experimental composite cement*

The light-cure experimental composite cement was composed of 2:1 (weight) UDMA and TEGDMA with the addition of 1 wt.% 4 N,N-trimethylanilin and 0.5 wt.% camphorquinone (Aldrich, Darmstadt, Germany) to initiate the photo-polymerization. After mixing, it was left for 24 h to stabilize. Silanated barium borosilicate (0.7 μm) was added at 22 parts of 100% of the organic mixture and amorphous organosilane-treated silica nano-fillers (40 nm) was added at 13 parts.

2.1.4. *Silane*

The experimental silane solution of 3-(trimethoxysilyl)propyl methacrylate (Aldrich, Darmstadt, Germany) (2 wt.%) was dissolved in 92.8 wt.% absolute ethanol, 5 wt.% deionized water and 0.2 wt.% acetic acid.

2.2. *Sample preparation*

2.2.1. *Prism manufacturing*

CAD-CAM blocks were cut at an angle of 60° with a low-speed saw (Isomet; Buehler, Lake Bluff, IL, USA) under continuous water irrigation to produce the prism-shaped samples, which were then wet-ground into the desired 14 ± 0.1 mm long triangular prisms, 6 ± 0.1 mm on a side with 220 grit silicon carbide (SiC) paper, at 300 rpm (Struers, Ballerup, Denmark) using a custom-built specimen holder. A total of 240 prisms were manufactured (120 PICN + 120 DF) which were split into two to produce the half prisms.

2.2.2. *Surface pre-treatment*

Bonded surfaces were polished with 1000 grit SiC paper to produce the equilateral 6 ± 0.1 mm long prisms. All samples were sonically cleaned in ethanol for 3 min then dried with oil-free dry air for 10 s. PICN and DF samples were then divided into two groups (n = 60 samples per group).

For the first group, 5% hydrofluoric acid (HF) (Vita ceramics etch, Vita Zahnfabrik, Bad Säckingen, Germany) was applied and left for 60 s, washed under running water for another 60 s, air dried, then sonically cleaned in ethanol for 3 min and again air dried.

For the second group, airborne-particle abrasion (AB) was performed using 50 μm Al_2O_3 particles (Danville, Zürich, Switzerland) for 5 s in a perpendicular direction at a distance of 1 cm from the sample at a pressure of 1 bar for PICN and

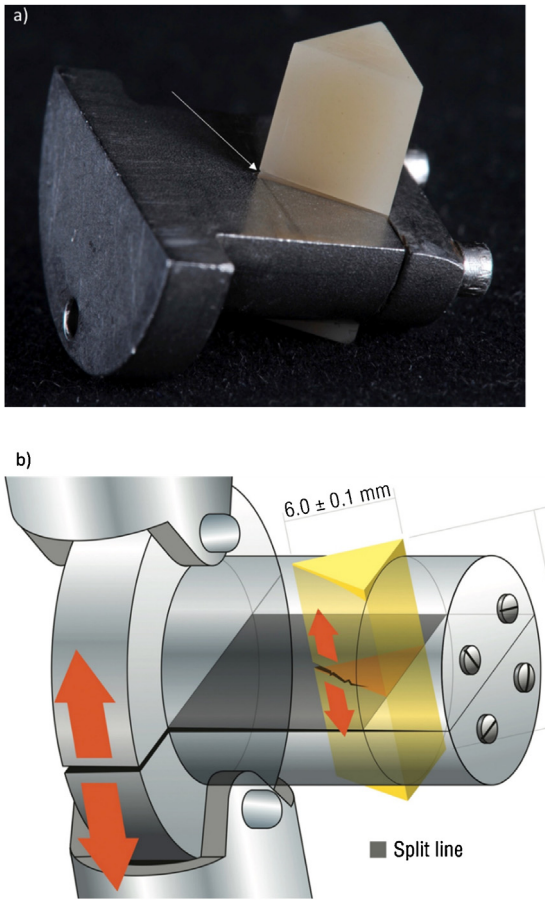

Fig. 2 – Notchless triangular prism (NTP) test. (a) A bonded prism fixed to one half of the cylindrical mounting block, with an arrow pointing at the crack initiation point. (b) A schematic illustration of the NTP apparatus in motion, with a bonded prism fixed within. The arrows pointing in opposite directions indicate the application of tensile force on the bonded interface, marked by the split line, with crack propagation starting from the tip of the prism at the crack initiation point until fracture or crack arrest. Figures were reprinted by permission of SAGE Publications Inc. from Eldafrawy et al. [11].

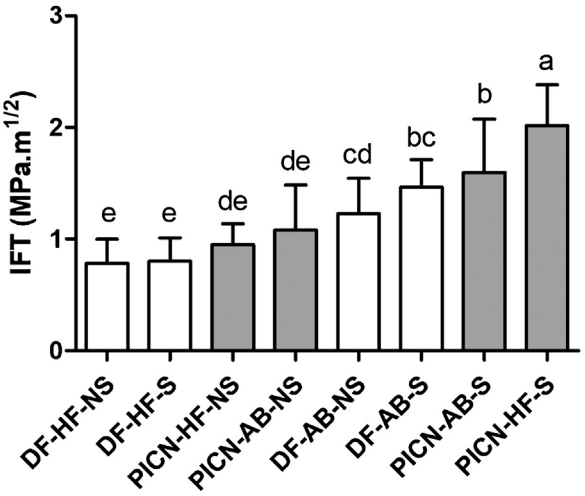

Fig. 3 – A bar graph of the interfacial fracture toughness (IFT) measurement. Results are expressed as the means ± SD. Superscript letters indicate statistically homogeneous subgroups within a material category (1-way ANOVA followed by Scheffé test, $\alpha = 0.05$). The same superscript letters demonstrate that there were no significant differences for each factor. PICN-HF-S is etched silanized PICN; PICN-AB-S is airborne-particle abraded silanized PICN; DF-AB-S is airborne-particle abraded silanized dispersed fillers; DF-AB-NS is airborne-particle abraded non-silanized dispersed fillers; PICN-AB-NS is airborne-particle abraded non-silanized PICN; PICN-HF-NS is etched non-silanized PICN; DF-HF-S is etched silanized dispersed fillers; DF-HF-NS is etched non-silanized dispersed fillers.

1.5 bar for DF. Samples were then sonically cleaned in ethanol for 3 min and air dried.

Each group was further divided into 2 sub-groups (n = 30 per sub-group); one sub-group receiving silane treatment (S), which was applied with a plastic brush and left for 60 s then dried with a stream of hot air (100 °C) for 30 s. The other sub-group was bonded immediately following surface pre-treatment.

2.2.3. *Bonding*

Half prisms were fixed into a custom-designed computer-controlled (SMC 100, Newport Corporation, California, USA) motorized alignment system (Newport Motion Controller) which controls the cement thickness at a precision of 0.1 μm, and the resin cement was applied on each of the pre-treated surfaces using a plastic spatula. Prisms were put into contact and the cement thickness was set to 50 μm. High power (1200 mW/cm^2) light applications were performed on each of the three sides of the prisms at close proximity (Bluephase 20i; Ivoclar Vivadent, Schaan, Liechtenstein) and an additional 40 s of curing was applied at a distance of 2 mm on each side after removal from the alignment apparatus to ensure optimal curing.

2.2.4. *Aging*

Samples were left for 24 h at 36 °C, 90% humidity (VCN 100, Vötsch Industrietechnik GmbH, Balingen, Germany), after which they were polished to remove excess resin cement using 1000 grit SiC, then submitted to thermocycling for 10,000 cycles at 5–55 °C, with a dwelling time of 30 s in each bath.

2.3. *Interfacial fracture toughness testing*

IFT was measured using the NTP test following the procedure described by Ruse et al. [36], in which samples were fixed into one half of the specimen holder and a crack initiation point (~0.1 mm) was made using a sharp scalpel under a light microscope at a magnification of ×20. After securing the other half of the specimens, samples were mounted on the computer-controlled (Bluehill, Instron Canada Inc., Burlington, ON) universal testing machine (Instron model 5565) within a water bath at 36 °C, at a cross-head speed of

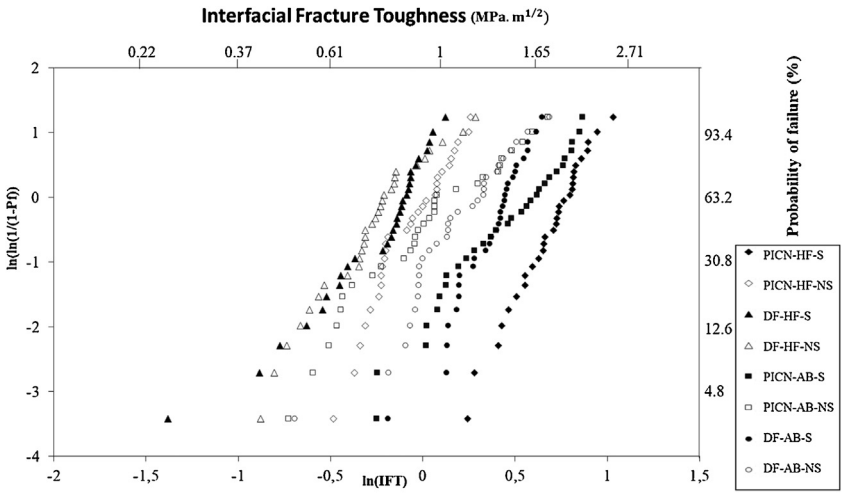

Group	PICN HF-S	PICN HF-NS	PICN AB-S	PICN AB-NS	DF HF-S	DF HF-NS	DF AB-S	DF AB-NS
Weibull modulus	5.9	5.5	3.5	2.9	3.3	3.9	6.1	4.0

Fig. 4 – Weibull plots of the interfacial fracture toughness (IFT) results. PICN-HF-S is etched silanized PICN; PICN-AB-S is airborne-particle abraded silanized PICN; DF-AB-S is airborne-particle abraded silanized dispersed fillers; DF-AB-NS is airborne-particle abraded non-silanized dispersed fillers; PICN-AB-NS is airborne-particle abraded non-silanized PICN; PICN-HF-NS is etched non-silanized PICN; DF-HF-S is etched silanized dispersed fillers; DF-HF-NS is etched non-silanized dispersed fillers.

0.05 mm/min (Fig. 2). The values of load were recorded at failure arrest in a tensile mode and IFT was calculated using the formula $K_{IC} = Y^*_{min}\ P_{max}/DW^{1/2}$, where P_{max} is the maximum load at failure, D is the NTP specimen diameter (12 mm), W is the NTP specimen length (10.5 mm) and Y_{min} is the dimensionless stress intensity factor coefficient minimum (28) as given by Ruse et al. [36].

All prisms were examined under the light microscope to determine the mode of failure. Adhesive failures are those with a crack propagating at the interface between the resin cement and the composite material, while in mixed failures the crack propagates at the interface but with small portions of composite material or resin cement in the fracture surface. In cohesive failures, the crack propagates only within the composite material and samples that fracture in a cohesive mode are excluded from the data analysis [11,25].

2.4. *Contact angle measurement*

Fifteen rectangular samples (17.5 × 14.0 × 4.0 mm) of PICN and DF, in addition to 10 samples of UDMA polymerized under HT-HP and a pure glass-ceramic represented by Vita Mark II (Vita Zahnfabrik), were manufactured and polished in the same way as described before. For PICN and DF, 5 samples were treated with HF, 5 with AB, following the previously described procedures of bonding, and 5 were not submitted to a surface treatment. For UDMA and Vita Mark II, only untreated and etched samples were analyzed (n = 5 per group). Samples were cleaned sonically in alcohol, air-dried and analyzed before and after silanization by measuring the contact angle of 3 drops of deionized water on the surface after 60 s (DSA-30, Kruss, Hamburg, Germany).

An identical set of samples were tested for contact angle measurement with a drop of TEGDMA instead of water.

2.5. *Developed interfacial area ratio*

Three rectangular samples of DF and PICN of the same dimensions as the ones used for contact angle measurement were manufactured and polished with 1000-grit SiC paper. Two of the samples were treated with HF and airborne-particle abrasion following the previously described procedures. The third sample was left untreated. Profilometry was carried out on the samples to measure the developed interfacial area ratio (Sdr), which is expressed as the percentage of additional surface area contributed by the texture compared to an ideal plane the size of the measurement region. The Sdr is obtained by calculating the topographical area with respect to this ideal plane and gives the surface enlargement induced by the different pre-treatments. Measurements were performed using an optical profiler (Contour GT-I; Bruker) in high-resolution vertical scanning inferometry (VXI) mode at <1 nm, independent of the objective. Five measurements were taken at the centre of each sample with a ×115 objective (image size: 0.06 × 0.04 mm^2; optical lateral resolution: 0.33 μm) with no filtering and removal of the tilt and cylinder terms. The values of the Sdr were obtained by calculating the mean of 5 values measured for each sample.

2.6. *SEM surface characterization*

Rectangular samples of PICN, DF, UDMA and Vita Mark II were manufactured and polished. For PICN and DF, one sample was treated with HF, one with airborne-particle abrasion

Table 1 – The results of a 3-way ANOVA of the interfacial fracture toughness (IFT). * indicates that a significant difference was detected ($p < 0.05$). Superscript letters indicate statistically homogenous sub-groups within a material category (Scheffé test, $\alpha = 0.05$). The same superscript letters demonstrate that there were no significant differences for each factor. The F-statistic column is labeled "F". Number of samples (n) = 30.

				IFT (MPa $m^{1/2}$)					
Factor				Mean ± SD (95% confidence interval)	df	Type III sum of squares	Mean square	F	Significance
M: material class	PICN			1.40 ± 0.58 [a] (1.34–1.46)	1	6.507	6.507	61.905	*
	DF			1.07 ± 0.21 [b] (1.01–1.13)					
ST: surface treatment	HF			1.14 ± 0.57 [b] (1.08–1.20)	1	2.205	2.205	20.971	*
	AB			1.33 ± 0.44 [a] (1.27–1.39)					
Si : Silane	Silane			1.47 ± 0.55 [a] (1.41–1.53)	1	13.431	13.431	127.765	*
	No silane			1.00 ± 0.34 [b] (0.94–1.05)					
M × ST	PICN	HF		1.48 ± 0.61 [a] (1.40–1.57)	1	7.896	7.896	75.117	*
		AB		1.31 ± 0.54 [a] (1.23–1.39)					
	DF	HF		0.79 ± 0.21 [b] (0.71–0.87)					
		AB		1.35 ± 0.31 [a] (1.26–1.43)					
M × Si	PICN	Silane		1.81 ± 0.47 [a] (1.72–1.89)	1	7.103	7.103	67.571	*
		No silane		0.99 ± 0.33 [b] (0.91–1.07)					
	DF	Silane		1.13 ± 0.40 [b] (1.05–1.22)					
		No silane		1.00 ± 0.35 [b] (0.92–1.09)					
ST × Si	HF	Silane		1.41 ± 0.68 [a] (1.33–1.49)	1	0.304	0.304	2.892	–
		No silane		0.86 ± 0.22 [c] (0.78–0.95)					
	AB	Silane		1.53 ± 0.38 [a] (1.45–1.61)					
		No silane		1.13 ± 0.39 [b] (1.05–1.21)					
M × ST × Si	PICN	HF	Silane	2.02 ± 0.37 [a] (1.90–2.13)	1	1.918	1.918	18.245	*
			No silane	0.95 ± 0.19 [de] (0.83–1.07)					
		AB	Silane	1.60 ± 0.48 [b] (1.48–1.71)					
			No silane	1.03 ± 0.43 [de] (0.91–1.15)					
	DF	HF	Silane	0.80 ± 0.21 [e] (0.69–0.92)					
			No silane	0.78 ± 0.22 [e] (0.66–0.90)					
		AB	Silane	1.46 ± 0.25 [bc] (1.35–1.58)					
			No silane	1.23 ± 0.32 [cd] (1.11–1.34)					

and the third sample was left untreated. For UDMA and Vita Mark II, only etched and untreated samples were prepared. Immediately following surface pre-treatment, each sample was cleaned sonically in ethanol for 3 min and subsequently gold-coated to be analyzed by scanning electron microscopy (SEM) (S-3000 N; Hitachi, Tokyo Japan).

2.7. SEM interface analysis

Four rectangular samples of each of PICN and DF, and 2 samples of Vita Mark II were manufactured and polished the same way described before. For PICN and DF, surface pre-treatments (HF and AB), with and without silane application, were carried out using the same protocol described for bonding. For Vita Mark II, only HF was applied. On each sample, a drop of experimental composite cement devoid of fillers was applied perpendicular to the surface and left for 60 s, then light-cured for another 60 s. Samples were then embedded in epoxy resin which was left to set for 24 h. The samples were then cut using a low-speed saw through the material/composite cement interface. They were then polished with 600 and 1000 grit SiC paper, then with a diamond pad and scanned by the SEM.

2.8. Statistical analysis

IFT and Sdr results were analyzed by one-way ANOVA followed, if warranted, by Scheffé multiple mean comparisons ($\alpha = 0.05$), using PASW Statistics 18 (SPSS, USA). Weibull statistics parameters were calculated for the IFT data using the Weibull statistics option in Excel (Microsoft, USA). The Weibull distribution was described in previous studies [38,39]. Two-way ANOVA was used to evaluate the influence of microstructure, surface pre-treatment and both combined on the Sdr, while 3-way ANOVA was used to evaluate the influence of microstructure, surface pre-treatment, silane and all three combined on the IFT. Pearson's tests were used to verify the presence of statistically significant correlations between the IFT and Sdr ($\alpha = 0.05$).

3. Results

3.1. IFT

The IFT values (mean and standard deviations) of the different groups, along with the statistical analysis, are summarized in Fig. 3. PICN-HF-S showed the highest IFT (2.02 ± 0.37 MPa $m^{1/2}$) significantly followed by PICN-AB-S (1.6 ± 0.48 MPa $m^{1/2}$). The lowest IFT values were shown by DF-HF with and without silane (0.8 ± 0.21 MPa $m^{1/2}$ and 0.78 ± 0.22 MPa $m^{1/2}$, respectively). Silane application was shown to have a significant effect on IFT for PICN but not for DF materials. All the samples failed in an adhesive or a mixed manner, no cohesive or pre-test failures were observed in any of the tested groups. The amount of adhesive (A) and mixed (M) failures were: DF-HF-NS (A/30, M/0); DF-HF-S (A/29, M/1); PICN-HF-NS (A/30, M/0); PICN-AB-NS (A/29, M/1); DF-AB-NS (A/30, M/0); DF-AB-S (A/27, M/3); PICN-AB-S (A/27, M/3); PICN-HF-S (A/26, M/4). Weibull analysis of the PICNs was higher when treated with HF than when treated with airborne-particle abrasion. In contrast to this, Weibull analysis of the DFs was higher when treated with airborne-particle abrasion than when treated with HF (Fig. 4). Three-way ANOVA highlighted the significant effect of material class, surface pre-treatment and silanization, as well as the significant effect of all three combined on the IFT with resin cement (Table1).

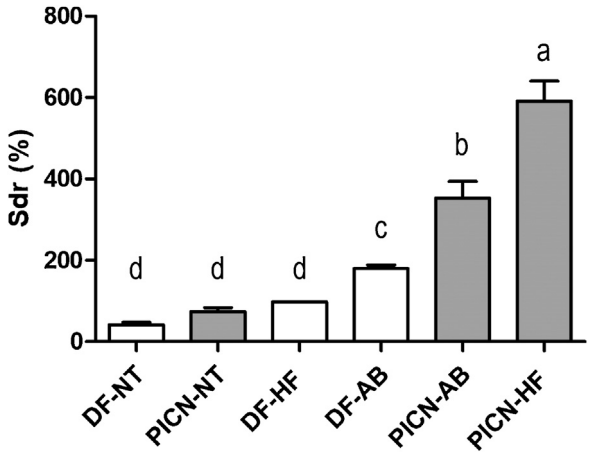

Fig. 5 – A bar graph of the developed interfacial area ratio (Sdr) measurement. Results are expressed as the means ± SD. Superscript letters indicate statistically homogeneous subgroups within a material category (1-way ANOVA followed by Scheffé test, $\alpha = 0.05$). The same superscript letters demonstrate that there were no significant differences for each factor. PICN-HF is etched PICN; PICN-AB is airborne-particle abraded PICN; DF-AB is airborne-particle abraded dispersed fillers; DF-HF is etched dispersed fillers; PICN-NT is PICN with no treatment; DF-NT is dispersed fillers with no treatment.

3.2. Sdr

The mean and standard deviations of the Sdr measurements for each group of samples, along with the results of the statistical analysis, are summarized in Fig. 5. PICN-HF showed the highest Sdr, significantly followed by PICN-AB, while there was no significant difference between DF-HF, PICN-NT and DF-NT. Images of profilometry are shown in Fig. 6.

Two-way ANOVA highlighted the significant effect of material class, surface pre-treatment and both combined on the Sdr (Table 2).

3.3. Correlation between the IFT and Sdr

Statistical analysis using Pearson's correlation coefficient revealed that there was a strong ($r^2 = 0.8411$) and significant ($p < 0.05$) correlation between the IFT of PICN and DF, when pre-treated with silane, and the Sdr. This positive correlation suggests that, under the conditions of this study, over 84% of the variation in the IFT was explained by the Sdr (Fig. 7). The correlation was found to be weaker when the non-silanized samples were included ($r^2 = 0.5918$).

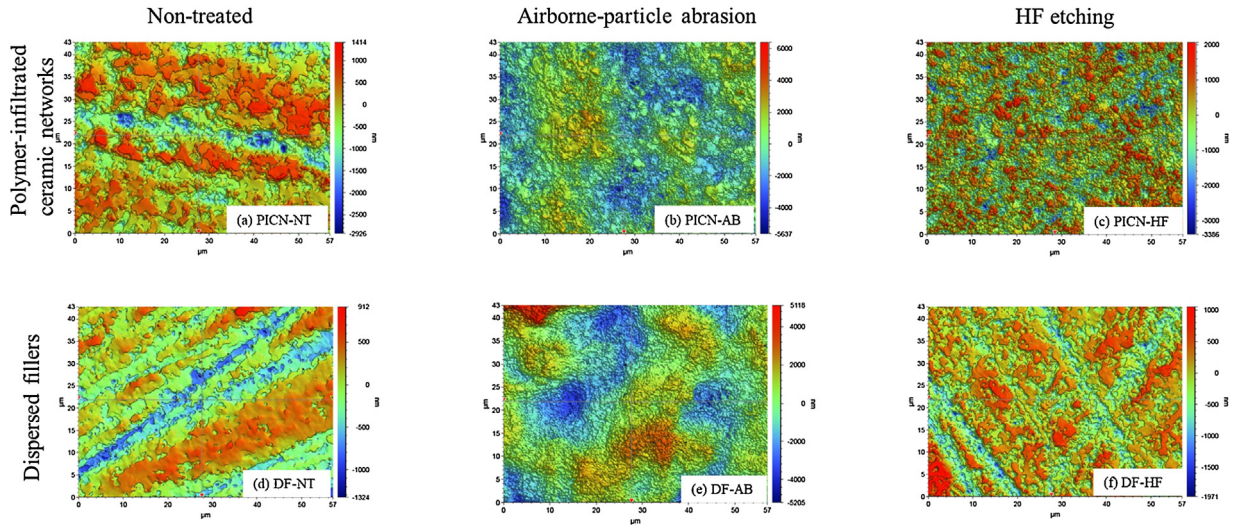

Fig. 6 – Profilometry images of the samples following different surface pre-treatments. The blue areas represent negative values, while the red areas represent positive values. (a) Non-treated PICN; (b) airborne-particle abraded PICN; (c) etched PICN; (d) Non-treated DF; (e) airborne-particle abraded DF; (f) etched DF. (For interpretation of the references to color in this figure legend, the reader is referred to the web version of this article.)

Table 2 – The results of a 2-way ANOVA of the developed interfacial area ratio (Sdr). * indicates that a significant difference was detected ($p < 0.05$). é test, $\alpha =$. The F-statistic column is labeled "F". Number of samples (n) = 30.

Sdr (%)								
Factor			Mean ± SD	df	Type III sum of squares	Mean square	F	Significance
M: material class	PICN		471.7 ± 132.5	1	522235,281	522235,281	465,157	*
	DF		143.2 ± 43.8					
ST: surface treatment	HF		371.5 ± 262.4	1	28503,800	28503,800	25,388	*
	AB		266.3 ± 95.3					
M*ST	PICN	HF	590.7 ± 49.9	1	120689,794	120689,794	107,499	*
		AB	352.8 ± 40.6					
	DF	HF	97.5 ± 1.1					
		AB	179.8 ± 8.6					

3.4. *Contact angle*

Contact angle measurements with water are displayed in Fig. 8. For DF, PICN and UDMA, surface pre-treatment with AB or HF increased the contact angle, i.e. lowered the wettability. On the other hand, following silane application, the contact angle was lowered, i.e. the wettability was increased. Conversely, Vita Mark II samples showed increased wettability after etching, and subsequent silane application decreased it. For contact angle measurement using TEGDMA, all the samples gave a zero value.

3.5. *SEM surface characterization*

SEM images of non-treated and etched PICN, DF, Vita Mark II and pure UDMA, as well as PICN and DF with airborne-particle abrasion are displayed in Fig. 9. The difference in microstructure between PICN and DF is shown in the non-treated samples, in which PICN, with its ceramic network, has a higher glass-ceramic density compared to DF, however sintering necks are difficult to highlight due to the presence of the polymer. Etching of PICN resulted in a specific microstructure of the surface, characterized by dissolution of the glass-ceramic network and the presence of a typical polymer-based honeycomb structure (Fig. 9b), including micro- and nano-porosities. On the other hand, HF did not create as much roughness on the surface of the DF as it did with PICN, while Vita Mark II showed marked dissolution of the glass-ceramic at the surface and there was no observable change on the surface of UDMA after etching. The effect of AB on both classes, PICN and DF, was very slight in comparison with HF.

3.6. *SEM interface analysis*

Fig. 10 shows the SEM images of the interface, highlighting the presence of gaps between glass-ceramic and composite cement on PICN-HF, PICN-AB, and etched Vita Mark II samples in comparison to their silanized counterparts. In contrast, such gaps were not highlighted on DF samples, whatever the type of pre-treatment.

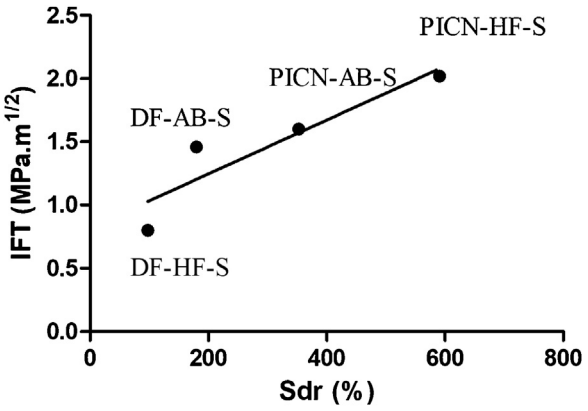

Fig. 7 – Interfacial fracture toughness (IFT) versus developed interfacial area ratio (Sdr) and their correlation curve ($r^2 = 0.8411$). Results are expressed as the means ± SD of IFT and Sdr for the tested samples of polymer infiltrated ceramic network (PICN) materials and dispersed filler (DF). PICN-AB-S is airborne-particle abraded silanized PICN; PICN-HF-S is etched silanized PICN; DF-AB-S is airborne-particle abraded silanized dispersed fillers; DF-HF-S is etched silanized dispersed fillers.

4. Discussion

The NTP test was successfully used to evaluate adhesive interfaces and the obtained results were shown to be within the same range of values compared to previous work using the same method to evaluate IFT of composite cement with PICN and DF CAD-CAM composites [11,15]. In the present work, the alignment system for half-prism bonding was improved to accurately control the cement thickness, which was set at 50 μm to be close to clinical situations [40,41]. AB pressure varied between the 2 materials because the authors followed the instructions of the commercially available products, Vita Enamic (Vita Zahnfabrik) for PICN and Cerasmart (GC) for DF. Thermocycling was performed following recent guidelines [42], with aging having an important influence on the reliability of adhesive interfaces due to hydrolytic degradation of the bonding interface [43]. The samples were tested in a water bath set at 36 °C to provide a close approximation of the in-mouth conditions and to eliminate any bias resulting from differences in temperature [31]. Finally, the use of experimental materials was intended to control material composition and microstructure.

According to this study, the material microstructure (PICN or DF) and the surface pre-treatment (HF or AB) were confirmed to significantly influence IFT with composite cement, hence the first and second null hypotheses were rejected [11]. PICNs were shown to perform significantly better than DF, with higher reliability as confirmed by Weibull analysis (Fig. 4), and showed higher IFT when etched, while DF should be pre-treated with airborne-particle abrasion, confirming previous results [11]. Material microstructure was previously shown to be a critical factor, which has an important influence on the bonding properties of CAD-CAM composites. The typical honeycomb polymer-based structure of PICN, when etched, was shown to exhibit significantly higher surface enlargement and consequently an increased chance of micromechanical bond (Figs. 5 and 9b). Silane application was shown to have a significant effect on IFT for PICN, but not for DF materials. A strong correlation between Sdr and IFT was found only when silane was applied, thus the third null hypothesis was rejected for PICN, but not for DF. One explanation is that, as described in literature [19], silane increases material surface wettability, which can promote composite cement spreading into the

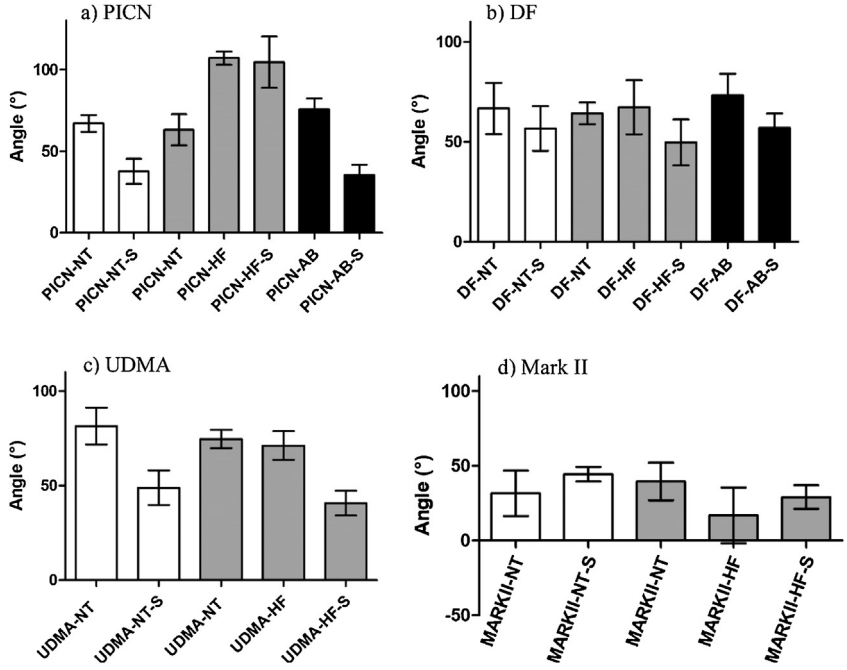

Fig. 8 – Bar graphs of the results of contact angle measurements. (a) PICN; (b) DF; (c) UDMA; (d) Vita Mark II. Bars with the same color represent the same sa-mple. Results are expressed as the means ± SD.

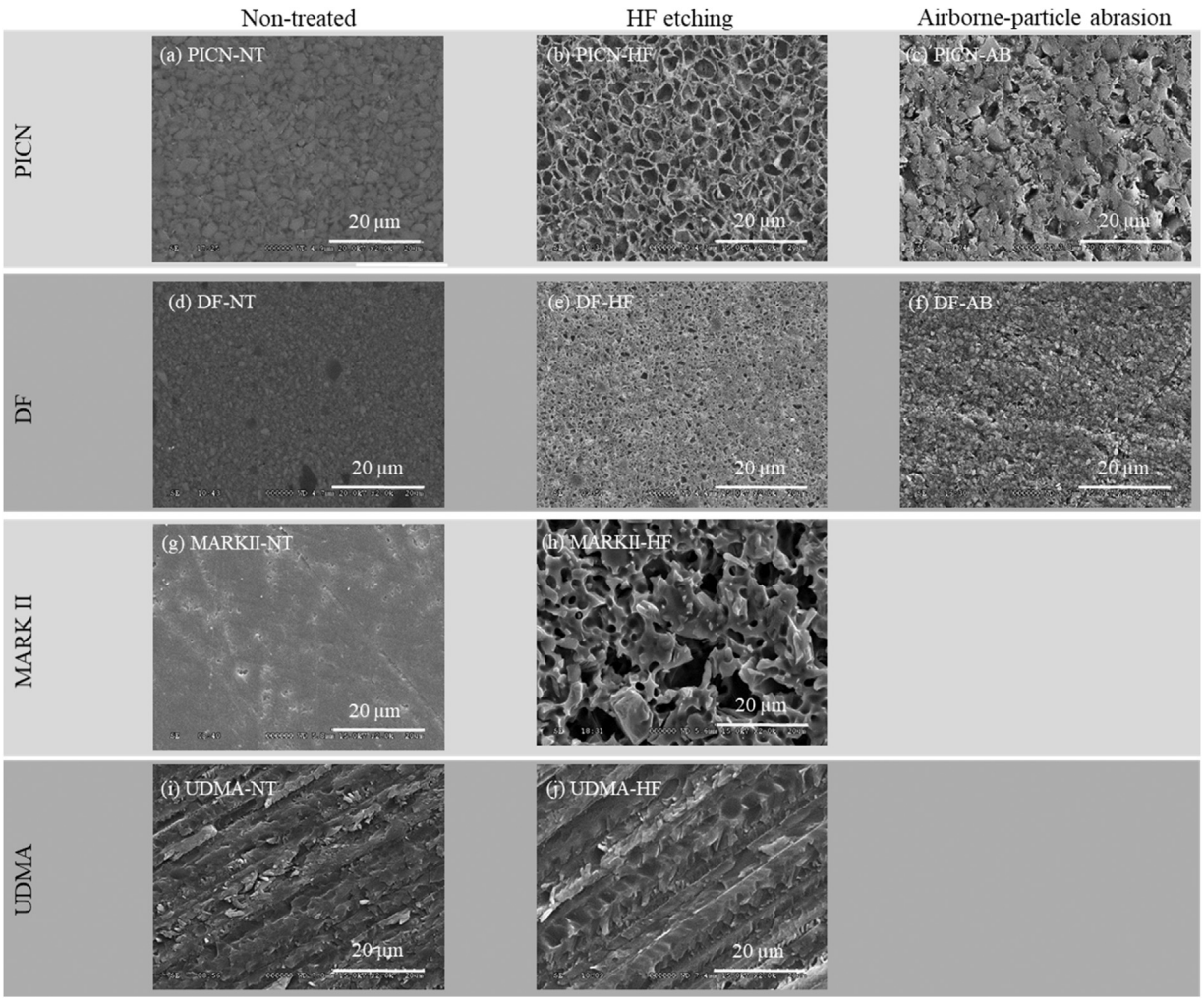

Fig. 9 – Scanning electron microscopy characterization of the samples following different surface pre-treatments. (a) Non-treated PICN; (b) etched PICN; (c) airborne-particle abraded PICN; (d) Non-treated DF; (e) etched DF; (f) airborne-particle abraded DF; (g) non-treated Mark II; (h) etched Mark II; (i) non-treated UDMA; (j) etched UDMA.

high surface roughness of PICN and consequently micromechanical bond. Indeed, contact angle measurements showed that if, as expected, surface HF or AB treatment decreased wettability with water of PICN, DF and UDMA, silane application increased it again in a significant way for all materials except for Vita Mark II. It must be noted that TEGDMA, with its low viscosity, was shown to spread readily on all the surfaces irrespective of the material, pre-treatment or silane application. The interface SEM observations (Fig. 10) support this explanation, highlighting the presence of gaps between glass-ceramic and composite cement on non-silanized PICN and glass-ceramic (Vita Mark II) samples. However, findings also support the second reported effect of silane [16,19], which is the creation of a chemical bond with glass-ceramics, also explaining the presence of gaps after composite cement polymerization and retraction. The slight decrease of wettability with silane application on the etched Vita Mark II sample surfaces, also promotes the hypothesis of the chemical bonding to explain silane positive effect on glass-ceramics [16,19]. In fact, the mode of action of silane is unclear and seems very complex. Its amphiphilic nature can explain its affinity for both the inorganic and organic parts of PICN and DF materials, as for water and TEGDMA, which could promote the energy increase of all surfaces.

Until now, few studies have evaluated the influence of silane pre-treatment on bonding properties of CAD-CAM composites with resin cement. DF and PICN represented by Lava Ultimate and Vita Enamic respectively, were tested for MTBS with 2 different composite resins, with etching and airborne-particle abrasion, with and without silane, for each type of pre-treatment [14]. When silane was applied, HF-PICN also gave better results than AB-DF or HF-DF, while there was no significant effect of silane on Lava Ultimate, as observed with DF in the present study. However, in a recent study on different DF CAD-CAM composites [44] the shear bond strength was significantly higher with sandblasting and silanization than with sandblasting alone, except for one material, which was attributed to damages induced by the sandblasting procedure. The positive influence of silane on the bond strength for PICN was also highlighted in a previous study conducted by Elsaka [13], in which the MTBS values, after aging in water for 30 days, were significantly higher when silane was

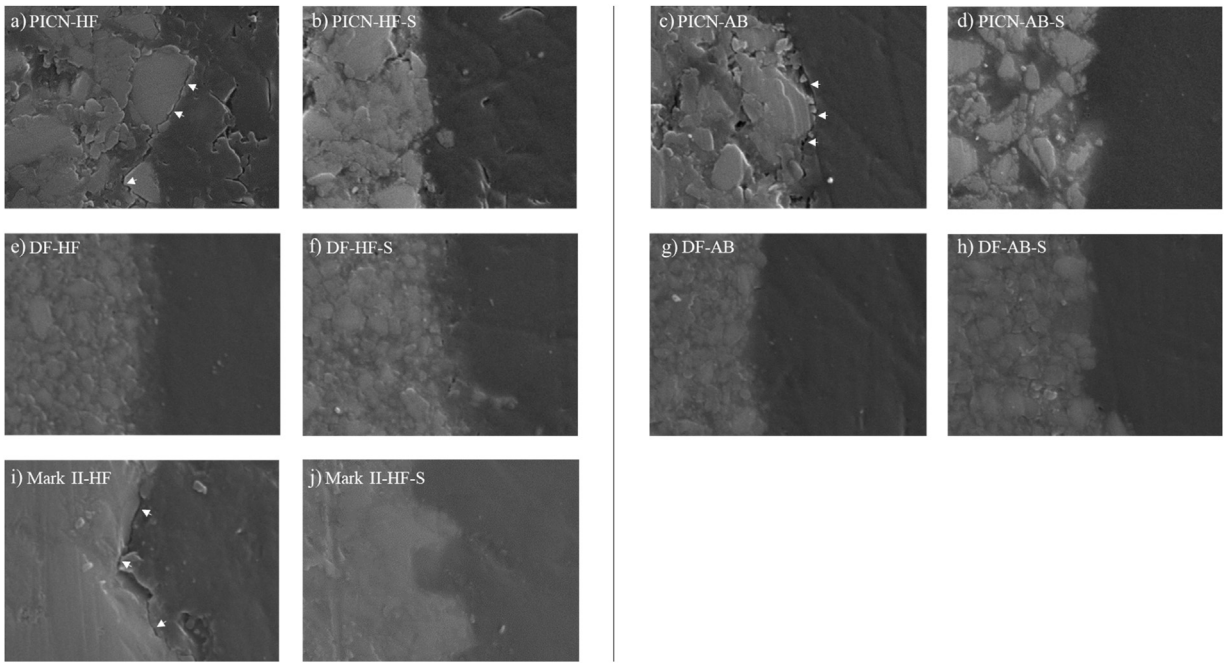

Fig. 10 – Scanning electron microscopy of the cement interface with PICN, DF and Vita Mark II. The arrows are pointing at areas of incomplete wettability. (a) Etched PICN; (b) etched silanized PICN; (c) airborne-particle abraded PICN; (d) airborne-particle abraded silanized PICN; (e) etched DF; (f) etched silanized DF; (g) airborne-particle abraded DF; (h) airborne-particle abraded silanized DF; (i) etched Vita Mark II; (j) etched silanized Vita Mark II.

applied than when the material was etched and bonded directly.

5. Conclusion

Silane increases bonding effectiveness of resin cement to PICNs but not to DF materials. Results of the present study highlight the importance of material microstructure and consequently surface properties on bonding effectiveness to composite cement. They suggest that silane improves micromechanical interlocking by promoting surface wettability and composite cement penetration in PICN high surface roughness when pre-treated. Indeed, PICNs, with their specific honeycomb microstructure when etched, exhibited significantly higher surface roughness, as shown by the Sdr values, and then IFT with composite cement than DF materials. Within the limitations of the present study, particularly slight differences in composition of experimental compared to marketed materials, results suggest that PICNs should perform better in terms of bonding properties than DF, and should be etched and silanized before resin cement application, while DF should be sandblasted and silanized, even if silanization is not as effective as with PICNs. Further research is needed to determine the exact effect silane has on the surface properties of CAD-CAM composite materials.

Acknowledgements

The authors received no financial support for this work. M.J. Sadoun has a patent: Composite ceramic block. US patent 8,507,578 B2. This research did not receive any specific grant from funding agencies in the public, commercial, or not-for-profit sectors.

REFERENCES

[1] Awada A, Nathanson D. Mechanical properties of resin-ceramic CAD/CAM restorative materials. J Prosthet Dent 2015;114(4):587–93.
[2] Lebon N, Tapie L, Vennat E, Mawussi B. Influence of CAD/CAM tool and material on tool wear and roughness of dental prostheses after milling. J Prosthet Dent 2015;114(2):236–47.
[3] Mainjot AKJ. The one step-no prep technique: a straightforward and minimally invasive approach for full-mouth rehabilitation of worn dentition using polymer-infiltrated ceramic network (PICN) CAD-CAM prostheses. J Esthet Restor Dent 2018. Epub ahead of print.
[4] Spitznagel FA, Horvath SD, Guess PC, Blatz MB. Resin bond to indirect composite and new ceramic/polymer materials: a review of the literature. J Esthet Restor Dent 2014;26(6):382–93.
[5] Mainjot AK, Dupont NM, Oudkerk JC, Dewael TY, Sadoun MJ. From artisanal to CAD-CAM blocks: state of the art of indirect composites. J Dent Res 2016;95:487–95.
[6] Sadoun M. inventorComposite ceramic block. US patent 8,507,578 B2; 2011.
[7] Nguyen JF, Migonney V, Ruse ND, Sadoun M. Properties of experimental urethane dimethacrylate-based dental resin composite blocks obtained via thermo-polymerization under high pressure. Dent Mater 2013;29(5):535–41.

[8] Nguyen JF, Ruse D, Phan AC, Sadoun MJ. High-temperature-pressure polymerized resin-infiltrated ceramic networks. J Dent Res 2014;93(1):62–7.
[9] Phan AC, Tang ML, Nguyen JF, Ruse ND, Sadoun M. High-temperature high-pressure polymerized urethane dimethacrylate-mechanical properties and monomer release. Dent Mater 2014;30(3):350–6.
[10] Spitznagel FA, Vuck A, Gierthmuhlen PC, Blatz MB, Horvath SD. Adhesive bonding to hybrid materials: an overview of materials and recommendations. Compend Contin Educ Dent 2016;37(9):630–7.
[11] Eldafrawy M, Ebroin MG, Gailly PA, Nguyen JF, Sadoun MJ, Mainjot AK. Bonding to CAD-CAM composites: an interfacial fracture toughness approach. J Dent Res 2018;97(1):60–7.
[12] Reymus M, Roos M, Eichberger M, Edelhoff D, Hickel R, Stawarczyk B. Bonding to new CAD/CAM resin composites: influence of air abrasion and conditioning agents as pretreatment strategy. Clin Oral Investig 2018;23:529–38.
[13] Elsaka SE. Bond strength of novel CAD/CAM restorative materials to self-adhesive resin cement: the effect of surface treatments. J Adhes Dent 2014;16(6):531–40.
[14] Frankenberger R, Hartmann VE, Krech M, Kramer N, Reich S, Braun A, et al. Adhesive luting of new CAD/CAM materials. Int J Comput Dent 2015;18(1):9–20.
[15] Mesmar S, Ruse ND. Interfacial fracture toughness of adhesive resin cement-lithium-disilicate/resin-composite blocks. J Prosthodont 2017;28:e243–51.
[16] Lung CY, Matinlinna JP. Aspects of silane coupling agents and surface conditioning in dentistry: an overview. Dent Mater 2012;28(5):467–77.
[17] Matinlinna JP, Lassila LV, Ozcan M, Yli-Urpo A, Vallittu PK. An introduction to silanes and their clinical applications in dentistry. Int J Prosthodont 2004;17(2):155–64.
[18] Matinlinna JP, Lung CYK, Tsoi JKH. Silane adhesion mechanism in dental applications and surface treatments: a review. Dent Mater 2018;34(1):13–28.
[19] Tian T, Tsoi JK, Matinlinna JP, Burrow MF. Aspects of bonding between resin luting cements and glass ceramic materials. Dent Mater 2014;30(7):e147–162.
[20] Campos F, Almeida CS, Rippe MP, de Melo RM, Valandro LF, Bottino MA. Resin bonding to a hybrid ceramic: effects of surface treatments and aging. Oper Dent 2016;41(2):171–8.
[21] Cekic-Nagas I, Ergun G, Egilmez F, Vallittu PK, Lassila LV. Micro-shear bond strength of different resin cements to ceramic/glass-polymer CAD-CAM block materials. J Prosthodont R 2016;60(4):265–73.
[22] Lise DP, Van Ende A, De Munck J, Vieira L, Baratieri LN, Van Meerbeek B. Microtensile bond strength of composite cement to novel CAD/CAM materials as a function of surface treatment and aging. Oper Dent 2017;42(1):73–81.
[23] Peumans M, Valjakova EB, De Munck J, Mishevska CB, Van Meerbeek B. Bonding effectiveness of luting composites to different CAD/CAM materials. J Adhes Dent 2016;18(4):289–302.
[24] Schwenter J, Schmidli F, Weiger R, Fischer J. Adhesive bonding to polymer infiltrated ceramic. Dent Mater J 2016;35(5):796–802.
[25] Scherrer SS, Cesar PF, Swain MV. Direct comparison of the bond strength results of the different test methods: a critical literature review. Dent Mater 2010;26(2):e78–93.
[26] Van Meerbeek B, Peumans M, Poitevin A, Mine A, Van Ende A, Neves A, et al. Relationship between bond-strength tests and clinical outcomes. Dent Mater 2010;26(2):e100–121.
[27] Wong ACH, Tian T, Tsoi JKH, Burrow MF, Matinlinna JP. Aspects of adhesion tests on resin-glass ceramic bonding. Dent Mater 2017;33(9):1045–55.
[28] Armstrong S, Geraldeli S, Maia R, Raposo LH, Soares CJ, Yamagawa J. Adhesion to tooth structure: a critical review of "micro" bond strength test methods. Dent Mater 2010;26(2):e50–62.
[29] De Munck J, Luehrs AK, Poitevin A, Van Ende A, Van Meerbeek B. Fracture toughness versus micro-tensile bond strength testing of adhesive-dentin interfaces. Dent Mater 2013;29(6):635–44.
[30] Pongprueksa P, De Munck J, Karunratanakul K, Barreto BC, Van Ende A, Senawongse P, et al. Dentin bonding testing using a mini-interfacial fracture toughness approach. J Dent Res 2016;95(3):327–33.
[31] Soderholm KJ. Review of the fracture toughness approach. Dent Mater 2010;26(2):e63–77.
[32] Della Bona A, Anusavice KJ, Mecholsky Jr JJ. Apparent interfacial fracture toughness of resin/ceramic systems. J Dent Res 2006;85(11):1037–41.
[33] Armstrong SR, Boyer DB, Keller JC, Park JB. Effect of hybrid layer on fracture toughness of adhesively bonded dentin-resin composite joint. Dent Mater 1998;14(2):91–8.
[34] Cesar PF, Della Bona A, Scherrer SS, Tholey M, van Noort R, Vichi A, et al. ADM guidance-ceramics: fracture toughness testing and method selection. Dent Mater 2017;33(6):575–84.
[35] Toparli M, Aksoy T. Fracture toughness determination of composite resin and dentin/composite resin adhesive interfaces by laboratory testing and finite element models. Dent Mater 1998;14(4):287–93.
[36] Ruse ND, Troczynski T, MacEntee MI, Feduik D. Novel fracture toughness test using a notchless triangular prism (NTP) specimen. J Biomed Mater Res 1996;31(4):457–63.
[37] Far C, Ruse ND. Effect of bleaching on fracture toughness of composite-dentin bonds. J Adhes Dent 2003;5(3):175–82.
[38] Bona AD, Anusavice KJ, DeHoff PH. Weibull analysis and flexural strength of hot-pressed core and veneered ceramic structures. Dent Mater 2003;19(7):662–9.
[39] Weibull W. A statistical distribution function of wide applicability. J Appl Mech 1951;18:293–7.
[40] Hung SH, Hung KS, Eick JD, Chappell RP. Marginal fit of porcelain-fused-to-metal and two types of ceramic crown. J Prosthet Dent 1990;63(1):26–31.
[41] Moraes RR, Boscato N, Jardim PS, Schneider LF. Dual and self-curing potential of self-adhesive resin cements as thin films. Oper Dent 2011;36(6):635–42.
[42] Armstrong S, Breschi L, Ozcan M, Pfefferkorn F, Ferrari M, Van Meerbeek B. Academy of Dental Materials guidance on in vitro testing of dental composite bonding effectiveness to dentin/enamel using micro-tensile bond strength (muTBS) approach. Dent Mater 2017;33(2):133–43.
[43] Lung CY, Botelho MG, Heinonen M, Matinlinna JP. Resin zirconia bonding promotion with some novel coupling agents. Dent Mater 2012;28(8):863–72.
[44] Yoshihara K, Nagaoka N, Maruo Y, Nishigawa G, Irie M, Yoshida Y, et al. Sandblasting may damage the surface of composite CAD-CAM blocks. Dent Mater 2017;33(3):e124–35.